scientific data

OPEN

DATA DESCRIPTOR

An fNIRS dataset for Multimodal Speech Comprehension in Normal Hearing Individuals and Cochlear Implant Users

András Bálint[1,2] ✉, Wilhelm Wimmer[2,3], Christian Rummel[4,5], Marco Caversaccio[1,2] & Stefan Weder[2]

Understanding cortical processing in cochlear implant (CI) users is crucial for improving speech outcomes. Functional near-infrared spectroscopy (fNIRS) provides a non-invasive, implant-compatible method for assessing cortical activity during speech comprehension. However, existing studies suffer from methodological heterogeneity and a lack of standardized datasets, limiting cross-study comparisons and generalizability. To address this gap, we present a multimodal fNIRS dataset comprising 46 CI users and 26 normal hearing controls. Participants completed a clinically relevant speech comprehension task using the German Matrix Sentence Test (OLSA) under speech-in-quiet, speech-in-noise, audiovisual and visual speech (i.e., lipreading) conditions. fNIRS recordings covered key cortical regions involved in speech processing, including the prefrontal, temporal, and visual cortices. Additionally, we provide detailed metadata, including patient history, hearing tests, behavioral measures, and spatially registered probe positions. This data descriptor aims to provide a comprehensive resource for investigating multimodal speech understanding in CI users. It enables researchers to explore cortical adaptations in prosthetic hearing, contributing to the refinement of CI rehabilitation strategies and advancing the understanding of auditory neuroplasticity.

Background & Summary

Disabling hearing loss is a leading cause of moderate to severe disability worldwide, affecting over 430 million individuals[1]. Cochlear implants (CIs) bypass the inner ear and directly stimulate the auditory nerve via electrical potentials, offering a solution to individuals who do not benefit from conventional hearing aids[2,3]. In terms of speech understanding, despite their proven efficacy, CI outcomes vary significantly due to factors that remain poorly understood[4–7].

Emerging evidence highlights the critical role of brain activation patterns (i.e., cortical factors) in CI outcomes. Investigating these factors under clinically relevant conditions is essential for understanding individual variability, predicting outcomes, and optimizing therapeutic interventions[4,5,8,9].

Functional near-infrared spectroscopy (fNIRS) is an ideal neuroimaging tool for investigating cortical activation patterns in CI patients. By measuring changes in oxygenated and deoxygenated hemoglobin concentrations (HbO and HbR), fNIRS provides a non-invasive method for assessing cortical hemodynamic activity. It is silent, non-invasive, radiation-free, and compatible with ferromagnetic implants, making it suitable for clinical populations, including patients with CIs. The measuring optical probes, affixed to the head via a cap, enable long-term recordings in diverse environments and are compatible with other imaging modalities, such as magnetic resonance imaging (MRI) and electroencephalography (EEG). fNIRS has been applied across numerous

[1]Hearing Research Laboratory, ARTORG Center for Biomedical Engineering Research, University of Bern, Bern, 3008, Switzerland. [2]Department of ENT - Head and Neck Surgery, Inselspital, Bern University Hospital, University of Bern, Bern, 3010, Switzerland. [3]Department of Otorhinolaryngology, Klinikum rechts der Isar, Technical University of Munich, Munich, Germany. [4]Support Center for Advanced Neuroimaging (SCAN), University Institute of Diagnostic and Interventional Neuroradiology, Inselspital, Bern University Hospital, University of Bern, Bern, 3010, Switzerland. [5]European Campus Rottal-Inn, Technische Hochschule Deggendorf, Max-Breiherr-Straße 32, Pfarrkirchen, D-84347, Germany. ✉e-mail: andras.balint@unibe.ch

clinical domains, including: attention deficit hyperactivity disorder (ADHD)[10], stroke rehabiliation[11], depression diagnostics[12], neurodegeneration and cognitive decline[13,14], hearing loss and speech outcome prediction[15–18], neurorehabiliation[19] and tinnitus assessment[20,21].

Although fNIRS holds great potential, research on cortical factors in CI patients is complex, and existing studies suffer from methodological heterogeneity and a lack of standardized datasets[22–30]. The brain networks supporting speech understanding in CI listeners remain poorly understood, partly due to the challenges of obtaining functional neuroimaging data in this population[31].

As a result, the number of available fNIRS datasets in adult CI populations is limited[22,23,32]. Shader *et al.* shared a dataset involving 12 newly implanted CI participants, measuring cortical responses above auditory and visual brain areas[33,34]. Sherafati *et al.* collected fNIRS data on 20 unilaterally implanted CI patients and normal hearing (NH) controls, focusing on brain regions supporting spoken word understanding[31]. Steinmetzger *et al.* shared an fNIRS-EEG dataset of 20 CI patients with single-sided deafness, focusing on voice pitch processing in temporal regions[35]. Anderson *et al.* shared a dataset including 17 CI patients and NH controls measured preoperatively in auditory related brain regions[30].

These datasets represent important contributions to field[30,31,33–35]. However, they focus on specific aspects of speech processing, thereby do not comprehensively address multimodal speech understanding. In particular, they do not cover all relevant cortical areas involved in audiovisual speech perception[31,33]. Moreover, these studies lack behavioral assessments during fNIRS acquisition and do not include spatial registration of probe positions[30,31,33–35].

In our approach, we emphasize the importance of conducting research under clinically relevant conditions. We adapted a clinical speech audiometric test (German Matrix Sentence Test, OLSA), to assess cortical processing under different speech understanding scenarios, including speech-in-quiet, speech-in-noise, audiovisual speech and visual speech (i.e., lipreading) conditions. This approach ensures comparability with clinical assessments and allows for a more comprehensive investigation of multimodal speech understanding. Our dataset covers key brain regions involved in audiovisual speech perception, including the prefrontal, temporal, and visual cortices. We incorporated objective (e.g., hearing tests) and behavioral parameters to improve the accuracy of data interpretation. Further, we conducted spatial registration of the optical probe positions to correct for anatomical differences across participants, improving the reliability of group-level analyses.

The dataset presented in this data descriptor includes 46 CI patients and 26 NH controls. It is valuable for researchers in the field of hearing research, seeking to explore the neural basis of prosthetic hearing rehabilitation with CIs.

Potential applications of this dataset include, but are not limited to (i) exploration of neural mechanisms underlying speech perception in CI users across different listening modalities, (ii) comparative studies between CI and NH individuals to better understand cortical adaptations and neuroplasticity in prosthetic hearing, (iii) correlational analyses linking brain responses with objective or behavioral parameters (e.g., listening effort, speech-in-noise performance), (iv) development and validation of new signal processing pipelines for fNIRS data, especially in clinical populations, (v) training of machine learning models to predict individual rehabilitation outcomes or listening effort from neural signals.

Methods

Ethics statement. This study adhered to the Declaration of Helsinki and received approval from the local ethics committee (KEK-Bern, BASED-ID 2020-02978). All participants provided written informed consent before their participation.

Participants. The dataset comprises 72 participants, including 46 CI users with varying levels of speech understanding and 26 NH controls. All participants had normal or corrected-to-normal vision and no history of neurological or psychiatric conditions, nor any brain injury.

As inclusion criteria, CI users met the criterion of pure-tone average (PTA) hearing thresholds exceeding 80 decibel hearing level (dB HL) in both ears, averaged across 500, 1000, 2000, and 4000 Hz, confirmed via pure-tone audiometry. During the study, CI users wore the audio processor on their better-hearing side, as determined by audiometric assessment or personal preference.

Study procedure. Each participant took part in a single study appointment, which lasted approximately 2 to 2.5 hours. The study was conducted in a sound-treated acoustic chamber. Participants completed questionnaires, hearing assessments, and performed a multimodal speech comprehension task while brain activity was measured by fNIRS (summarized in Table 1). The score range and interpretation of the collected metadata are summarized in Table 2.

The study procedure involved:

- Step 1: Initial questionnaires to assess handedness, lipreading experience, and subjective hearing perception.
- Step 2: Pure-tone and speech audiometry to assess hearing.
- Step 3 and 5: fNIRS measurements involving multimodal speech comprehension task.
- Step 4 and 6: Behavioral assessments of listening effort, fatigue, and task engagement.
- Step 7: Spatial registration of probe positions.

Questionnaires. Before the neuroimaging experiment, participants completed questionnaires on their handedness (Edinburgh Handedness Inventory[36]), subjective hearing experience (SSQ-12[37]), and lipreading skills[38].

Step:	1 Qs*	2 Hearing tests	3 fNIRS task	4 Qs*	5 fNIRS task	6 Qs*	7 Spatial registration
Reported Data:							
Handedness	+						
Lipreading	+						
SSQ-12	+						
WRS		+					
SRT		+					
Fatigue	+			+		+	
ACALES				+		+	
Focus				+		+	
TRI				+		+	
SITUT				+		+	
ED				+		+	
fNIRS			+		+		
3D							+

Table 1. Study Procedure. Qs*: Questionnaires. SSQ-12: Qualities of Hearing, Spatial Hearing, Speech Hearing[37]. WRS: Word recognition score at 65 dB SPL[39]. SRT: Speech reception threshold in 65 dB SPL background noise[40,41]. Fatigue: Average of Rating of Fatigue Scale[51]. ACALES: Average of Adaptive Categorical Listening Effort Scaling[50]. Focus: Sum of Task Attention reports[52,53]. TRI: Sum of Task-Related Interference reports[52,53]. SITUT: Sum of Stimulus-Independent and Task-Unrelated Thoughts reports[52,53]. ED: Sum of External Distraction reports[52,53] fNIRS: Raw data recorded during fNIRS task. 3D: Probe positions recorded during spatial registration[54].

Name	Score Range and Interpretation
Clinical Questionnaires & Behavioral assessments	
Edinburgh Handedness Inventory[36]	Left, Right or Ambidextrous
Adaptive Categorical Listening Effort Scaling (ACALES)[50]	max: 13 - extreme effort min: 1 - no effort
Rating-of-Fatigue Scale[51]	max: 10 - total fatigue min: 0 - not fatigued at all
Task related attention, mind-wandering[52,53]	Categorical responses, reported twice: - Focused - Task-Related Interference (TRI) - Stimulus-Independent and Task -Unrelated Thoughts (SITUT) - External Distraction (ED)
Short form of the Speech, Spatial and Qualities of Hearing scale (SSQ-12)[37]	12 items, scored 0-10 per item, grouped into subscales: - Speech hearing - Spatial hearing - Qualities of hearing
Lipreading experience[38]	
(1) Proficiency at lipreading	max: 10 - I am a professional min: 0 - I can not read lips
(2) In everyday life, lipreading is an essential part of my understanding of language.	max: 5 - always true min: 1 - not true at all
(3) When do you read lips?	Categorical: 1- Never 2- In acoustically difficult situations 3- I always read lips (if possible)
(4) When people wear a mask, I have more trouble understanding the language.	max: 5 - always true min: 1 - not true at all
Hearing tests	
Pure-tone average (PTA) hearing thresholds in dB HL	high PTA - worse hearing sensitivity low PTA - better hearing sensitivity
Speech reception threshold (SRT) in 65 dB SPL noise[40–44]	high SRT - poorer speech understanding low SRT - better speech understanding
Word recognition score (WRS) at 65 dB SPL[39]	max: 100% - all words correctly recognized min: 0% - no words understood

Table 2. Summary of questionnaires, hearing tests, and behavioral assessments included in the metadata.

Hearing tests and etiology. All participants underwent speech audiometric testing. Speech recognition in quiet was assessed using the Freiburg monosyllabic word test at 65 dB sound pressure level (SPL), with word

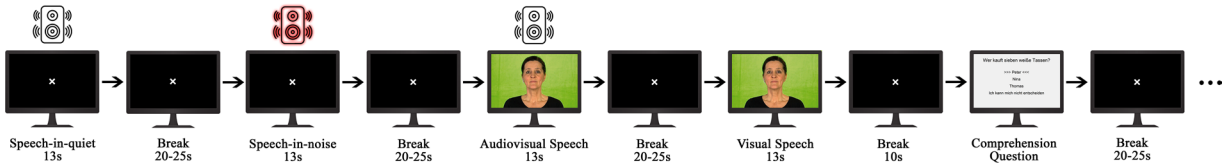

Fig. 1 The sentences were presented in either of the following conditions: speech-in-quiet, speech-in-noise, audiovisual speech, or visual speech. They were arranged in a counterbalanced block design, including a comprehension question about the content.

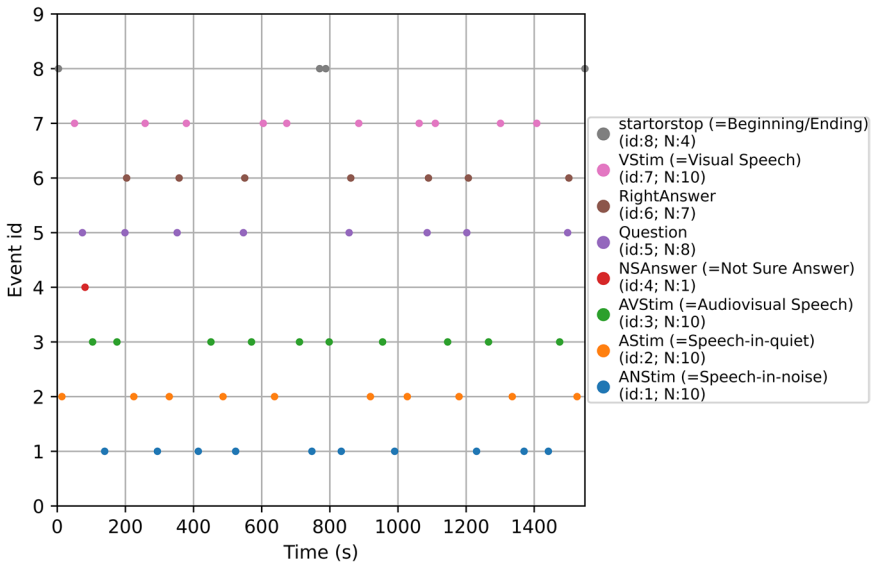

Fig. 2 Example timeline of the complete fNIRS measurement stored in the SNIRF files. The fNIRS task began with a start trigger, followed by ten counterbalanced blocks. These blocks consisted of four different listening conditions and two comprehension questions per condition. The questions had three possible outcomes: Right Answer, Wrong Answer, or Not Sure. After the fifth block, participants had a break, marked with a stop trigger.

recognition scores (WRS) reported as percentages[39]. Speech recognition in noise was evaluated using the adaptive OLSA[40–44], from which the speech reception threshold (SRT) was determined in dB sound-to-noise ratio (SNR). The maximum SNR was limited to 30 dB to avoid loudspeaker distortion.

For CI users, patient history included information on age at onset of deafness, duration of deafness, age at implantation, implant experience and cause of hearing loss. These variables are shared in an aggregated format in order to comply with the legal and ethical guidelines on human subject data.

fNIRS system and data acquisition. We used a continuous-wave fNIRS system (FOIRE-3000, Shimadzu, Kyoto, Japan) with 16 light sources and 16 detectors. The system emits laser light at wavelengths of 780 nm, 805 nm, and 830 nm, and a multi-alkali photomultiplier detector captures changes in the light's intensity.

To account for CI participants, the measurement probes were arranged to allow the attachment of the external CI transmitter behind the ear. The cap design included measurement channels above temporal, visual, and prefrontal brain regions. Three channels were short source-detector separation (SDS) channels to capture extracerebral signals[45–47]. The sampling rate was 14 Hz.

During the fNIRS measurement, participants were seated in a chair behind a desk with a monitor and a loudspeaker. The loudspeaker was calibrated to 65 dB SPL for all stimuli. Following task instructions and familiarization, the fNIRS cap was fitted to the participant's head. For CI users, any probes interfering with the external transmitter were removed.

fNIRS task design. In fNIRS tasks participants listened to sentences from the clinically established OLSA test[48]. Each 13-second long stimulus[49] consisted of a sentence repeated three times in one of four modalities: (1) speech-in-quiet (fixation cross only), (2) speech-in-noise (fixation cross only), (3) audiovisual speech (without noise), or (4) visual speech (i.e., lipreading). Each block included four stimuli (one per modality) and a comprehension questions about the content. Breaks of 20–25 seconds followed each

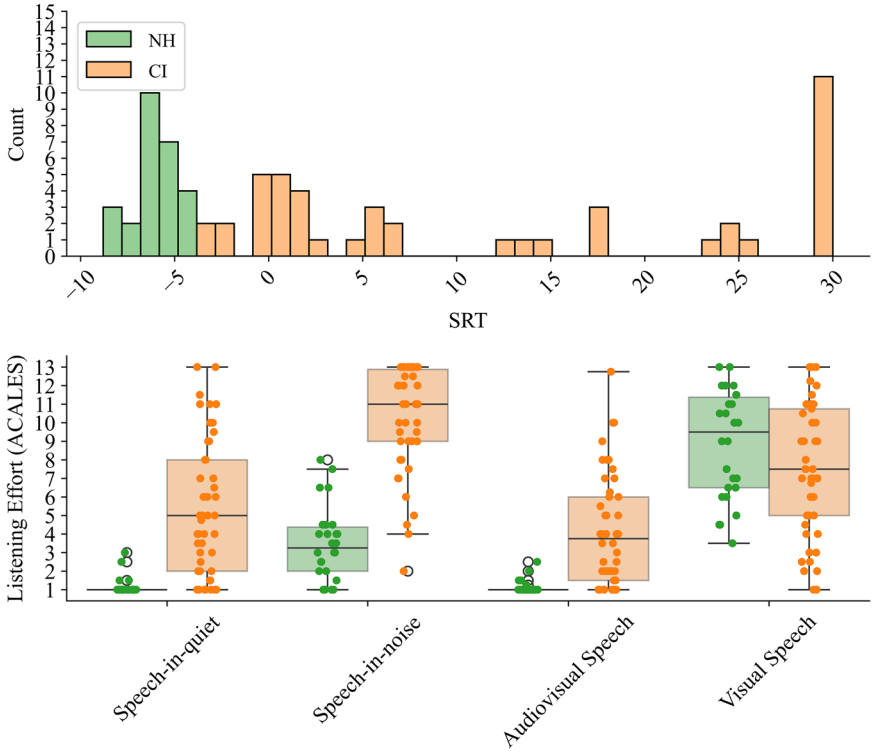

Fig. 3 Example variables from the audiological and behavioral assessments between normal hearing (controls, NH) and cochlear implant (CI) participants: The top row is the participant distribution by speech reception threshold (SRT), and the bottom row is the reported listening effort based on the Adaptive Categorical Listening Effort Scaling (ACALES). The box plot shows the median, quartiles, data range, and any outliers.

stimulus, shortened to 10 seconds before comprehension questions, with no time limit for answering (see the block design on Fig. 1).

Overall, participants completed ten counterbalanced blocks, resulting in ten repetitions and two questions per modality. After the fifth block, participants had an extended break to report on behavioral parameters.

Behavioral assessments. We collected behavioral data throughout the experiment to assess task-related parameters, including listening effort according to the Adaptive Categorical Listening Effort Scaling (ACALES)[50], fatigue measured using the Rating-of-Fatigue Scale[51] and task related attention or mind-wandering[52,53].

Spatial registration. Following the fNIRS task, we performed the spatial registration of the optical probe positions on the head using a Structure Sensor Pro 3D scanner (Occipital Inc., Boulder, United States) mounted to an iPad Pro 2020 (Apple Inc., Los Altos, California, United States, iOS 14.3)[54].

Data Records

The data are available at Dryad[55]. The dataset is organized according to the Brain Imaging Data Structure v1.10.0 (BIDS)[56] with the extension for NIRS data[57].

The main data files are stored in the Shared Near Infrared Spectroscopy Format (SNIRF)[58], a widely accepted standard for storing fNIRS data. The SNIRF files contain raw absorbance data from each channel at wavelengths of 780 nm, 805 nm, and 830 nm. They also include probe positions, and associated metadata from questionnaires, hearing tests, behavioral assessments, and patient history.

The temporal structure of each recording is consistent across participants and is illustrated in Fig. 2, which shows a representative example from a single participant. The fNIRS task begins with a start trigger, followed by ten counterbalanced blocks, with a break period at halftime.

Each participant has an individual SNIRF file, and also fields from the BIDS specification. The BIDS fields are replicated from the SNIRF file, which allows relevant behavioral, events or channel related data to be parsed without using an SNIRF reader. The latest specifications of the BIDS-NIRS format can be accessed online[59].

Participant-level information is stored in the root directory of the dataset in a “participants.tsv” file, along with an accompanying “participants.json” sidecar that provides descriptions of each column, following BIDS formatting conventions[60]. These are top level files summarizing relevant demographic and audiometric variables, enabling researchers to filter participant groups efficiently. To complement this, a more detailed Excel file (participants info.xlsx) include all metadata, with accompanying code provided in ”supplementary code” folder in MATLAB[61].

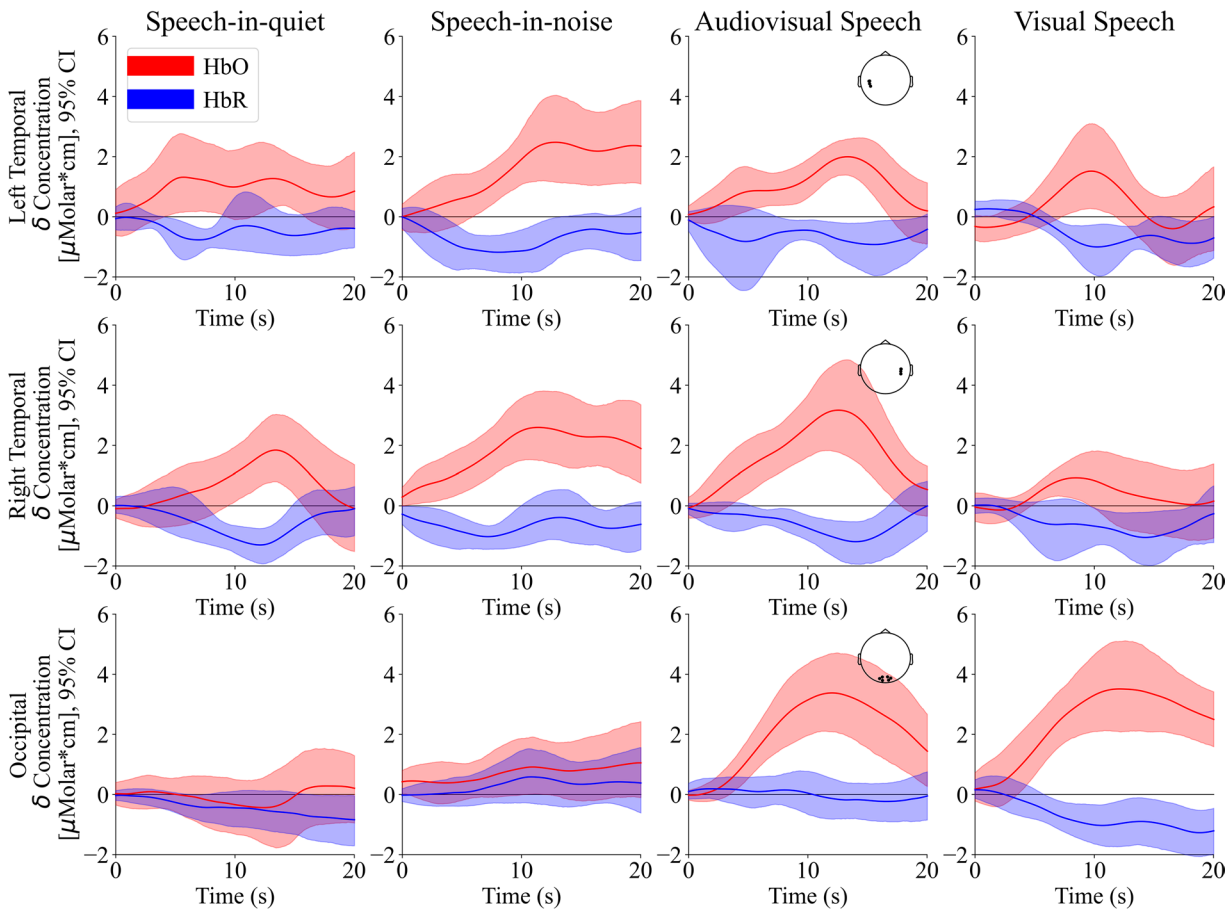

Fig. 4 Grand average evoked responses in three selected regions of interest (ROIs) for each condition. The red signal represents the concentration change in oxygenated hemoglobin (HbO) and the blue signal in deoxygenated hemoglobin (HbR). Error bars represent the 95% confidence intervals. The signals are measured in the normal hearing (NH) participants, who are serving as controls. In the top right corner, we show the channel positions which were included in the corresponding ROI, indicating the brain regions contributing to the grand average patterns. An increase in HbO and a decrease in HbR concentration indicate typical hemodynamic responses.

For Python, we provide a demonstration pipeline that includes loading, preprocessing, and visualization, implemented in a Jupyter Notebook (ds_main.ipynb) and a supporting script (ds_helpers.py). To run the demonstration, all dependencies listed in the "environment.yml" file needs to be installed.

Technical Validation

The data descriptor includes three main groups of data: (1) metadata, (2) raw fNIRS data, and (3) spatial registration data.

We report the (1) metadata without processing. We share the (2) raw fNIRS data in a BIDS-compliant format, and additionally we provide scripts for processing and visualization. We processed and visualized the (3) spatial registration data according to Bálint *et al.*[54].

fNIRS data processing. We used the MNE-NIRS toolbox for fNIRS data processing[62,63]. In the first step, we conducted short-separation regression on the raw absorbance data using the nearest short SDS channel[46,64,65]. The signal was then bandpass filtered in the range of 0.01-0.1 Hz[66].

Following, we converted to changes in HbO and HbR concentrations according to the specifications of the fNIRS machine (resulting unit µMolar*cm[67]):

$$\delta HbO = (-1.4887) * Abs^{780} + 0.5970 * Abs^{805nm} + 1.4878 * Abs^{830nm} \quad (1)$$

$$\delta HbR = 1.8545 * Abs^{780nm} - 0.2394 * Abs^{805nm} - 1.0947 * Abs^{830nm} \quad (2)$$

Motion artifacts were removed using temporal derivative distribution repair (TDDR)[68].

Individual epochs from 0 to 24 seconds following the onset of stimulation were extracted and baseline corrected (−5 to 0 seconds). Epochs in which participants reported interference (e.g., movement during stimulus

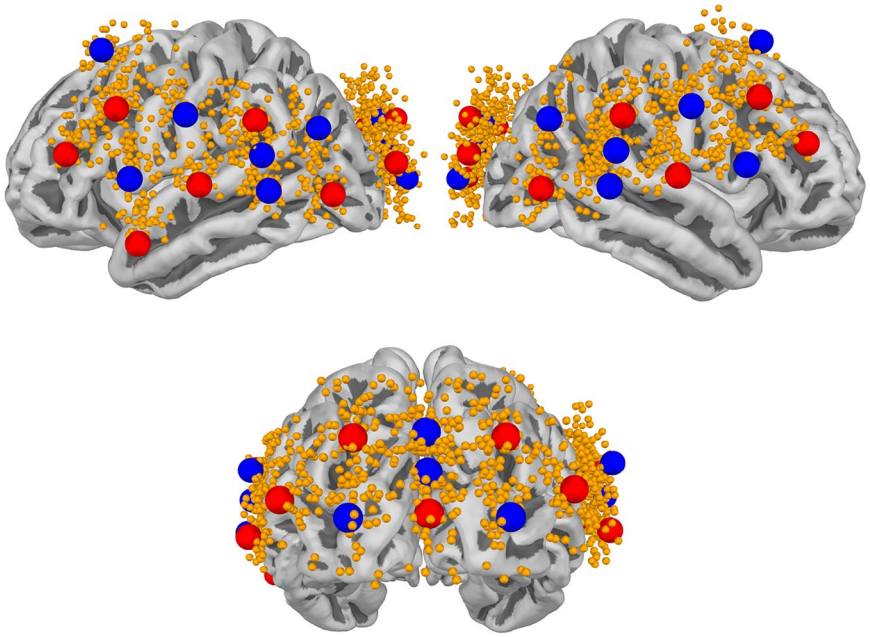

Fig. 5 Visualization of spatially registered probe positions. The top left is the lateral, the top right is the medial, and bottom middle is the caudal view. Yellow markers represent all registered positions, while red dots denote light sources and blue dots denote detectors for a single participant.

presentation, incorrectly selected answers) were removed, which affected 0.29% of all epochs. In addition, due to physical constraints from the CI coil, and cap setup, a subset of channels (4.5% of all channels) were marked as NaNs, meaning they were not used in the analysis.

Spatial registration processing. On the 3D scans, we manually labeled the probe positions and anatomical landmarks (nasion, left and right preauricular points) using MeshLab (version 2022.02)[69]. These labeled probe positions were then aligned with the MNE-Python 10-05 template[62,63] through rigid registration, using the anatomical landmarks as control points[54]. The resulting 3D positions are provided in the coordinate system of the MNE 10-05 template. In 14 NH and 9 CI cases out of 72 participants the spatial registration was insufficient, and data from a comparable participant with a matching head circumference was used. On average, a matching head size could be found within an error of 0.39 cm (standard deviation = 0.30 cm, range = 0-1.25 cm). These participants are marked in the dataset with the variable "HeadSizeMatch".

Metadata results. Figure 3 shows two examples from the metadata. The top row shows the distribution of participants based on their SRT. For NH participants, the values are consistent with normative data[70]. Some CI participants had an SRT comparable to those of the NH group, while others performed above this level (which means worse speech understanding in noise).

The bottom row shows listening effort ratings across different conditions during the fNIRS speech comprehension task. As expected due to their lower speech understanding, CI participants reported higher listening effort in speech-in-quiet, speech-in-noise, and audiovisual conditions compared to NH participants (top row). In the visual speech (i.e., lipreading) condition, CI participants showed effort across a wide range, with a trend towards reporting lower effort compared to NH participants.

fNIRS data results. The neurophysiological basis of fNIRS lies in the detection of local hemodynamic responses which reflects neural activity. In an activated brain region the blood flow increases more than oxygen metabolism, leading to changes in hemoglobin concentration[71]. Typically, an increase in HbO and a corresponding decrease in HbR concentration indicate a canonical hemodynamic response. The fNIRS signal is inherently slow, peaking multiple seconds after stimulation[72].

Figure 4 shows grand average evoked hemodynamic responses for three selected regions of interest (ROIs) across conditions in the NH group. Distinct activation patterns were observed: speech-in-quiet and speech-in-noise activated bilateral temporal ROIs, visual speech stimuli engaged mainly the occipital ROI, and audiovisual stimuli activated all ROIs. Channel positions contributing to each ROI are shown in the top right corner .

Spatial registration results. We have visualized the registered probe positions on Fig. 5, showing lateral, caudal and medial views. The yellow dots represent all of the registered positions. The red dots represent the light sources, while the blue dots represent the light detectors for a single participant. The cap design ensured coverage of key audiovisual speech regions, including the occipital cortex, left and right temporal cortices, and prefrontal areas.

Code availability

The code is available at Dryad[55].

Received: 1 April 2025; Accepted: 18 July 2025;
Published online: 26 July 2025

References

1. Organization, W. H. *et al*. World report on hearing. World Health Organization (2021).
2. Bond, M. *et al*. The effectiveness and cost-effectiveness of cochlear implants for severe to profound deafness in children and adults: a systematic review and economic model. *Health technology assessment* **13**(44), 1–196 (2009).
3. Carlson, M. L. Cochlear implantation in adults. *New England Journal of Medicine* **382**(16), 1531–1542 (2020).
4. Lazard, D. S. *et al*. Pre-, per-and postoperative factors affecting performance of postlinguistically deaf adults using cochlear implants: a new conceptual model over time. *PloS one* **7**(11), 48739 (2012).
5. Blamey, P. *et al*. Factors affecting auditory performance of postlinguistically deaf adults using cochlear implants: an update with 2251 patients. *Audiology and Neurotology* **18**(1), 36–47 (2012).
6. Kral, A., Aplin, F. & Maier, H. Prostheses for the Brain: Introduction to Neuroprosthetics. Academic Press (2021).
7. Bálint, A., Wimmer, W., Caversaccio, M., Rummel, C. & Weder, S. Linking brain activation to clinical outcomes: An fnirs study in cochlear implant users and normal hearing individuals. (Neurophotonics) (2025).
8. McKay, C. M. Brain plasticity and rehabilitation with a cochlear implant. *Advances in Hearing Rehabilitation* **81**, 57–65 (2018).
9. Lawrence, R. J., Wiggins, I. M., Anderson, C. A., Davies-Thompson, J. & Hartley, D. E. Cortical correlates of speech intelligibility measured using functional near-infrared spectroscopy (fnirs). *Hearing research* **370**, 53–64 (2018).
10. Poliakova, E., Conrad, A. L., Schieltz, K. M. & O'Brien, M. J. Using fnirs to evaluate adhd medication effects on neuronal activity: A systematic literature review. *Frontiers in neuroimaging* **2**, 1083036 (2023).
11. Huo, C. *et al*. A review on functional near-infrared spectroscopy and application in stroke rehabilitation. *Medicine in Novel Technology and Devices* **11**, 100064 (2021).
12. Ho, C. S. *et al*. Diagnostic and predictive applications of functional near-infrared spectroscopy for major depressive disorder: a systematic review. *Frontiers in psychiatry* **11**, 378 (2020).
13. Yang, D., Hong, K.-S., Yoo, S.-H. & Kim, C.-S. Evaluation of neural degeneration biomarkers in the prefrontal cortex for early identification of patients with mild cognitive impairment: an fnirs study. *Frontiers in human neuroscience* **13**, 317 (2019).
14. Pinti, P. *et al*. The present and future use of functional near-infrared spectroscopy (fnirs) for cognitive neuroscience. *Annals of the new York Academy of Sciences* **1464**(1), 5–29 (2020).
15. Bálint, A., Wimmer, W., Rummel, C., Caversaccio, M. & Weder, S.: Neural correlates of speech comprehension in normal hearing individuals and cochlear implant users-an fnirs study in quiet and noisy environments. In: *2024 46th Annual International Conference of the IEEE Engineering in Medicine and Biology Society (EMBC)*, pp. 1–5 IEEE (2024).
16. Weder, S., Zhou, X., Shoushtarian, M., Innes-Brown, H. & McKay, C. Cortical processing related to intensity of a modulated noise stimulus—a functional near-infrared study. *Journal of the Association for Research in Otolaryngology* **19**(3), 273–286 (2018).
17. Weder, S. *et al*. Cortical fnirs responses can be better explained by loudness percept than sound intensity. *Ear and hearing* **41**(5), 1187–1195 (2020).
18. Bálint, A. *et al*. Neural activity during audiovisual speech processing: Protocol for a functional neuroimaging study. *JMIR research protocols* **11**(6), 38407 (2022).
19. Mihara, M. & Miyai, I. Review of functional near-infrared spectroscopy in neurorehabilitation. *Neurophotonics* **3**(3), 031414 (2016).
20. Shoushtarian, M. *et al*. Objective measurement of tinnitus using functional near-infrared spectroscopy and machine learning. *PLoS One* **15**(11), 0241695 (2020).
21. Shoushtarian, M., Esmaelpoor, J., Bravo, M. M. & Fallon, J. B. Cochlear implant induced changes in cortical networks associated with tinnitus severity. *Journal of Neural Engineering* **21**(5), 056009 (2024).
22. Harrison, S. C., Lawrence, R., Hoare, D. J., Wiggins, I. M. & Hartley, D. E. Use of functional near-infrared spectroscopy to predict and measure cochlear implant outcomes: A scoping review. *Brain Sciences* **11**(11), 1439 (2021).
23. Farrar, R., Ashjaei, S. & Arjmandi, M. K. Speech-evoked cortical activities and speech recognition in adult cochlear implant listeners: a review of functional near-infrared spectroscopy studies. *Experimental Brain Research* **242**(11), 2509–2530 (2024).
24. Chen, L.-C., Stropahl, M., Schönwiesner, M. & Debener, S. Enhanced visual adaptation in cochlear implant users revealed by concurrent eeg-fnirs. *Neuroimage* **146**, 600–608 (2017).
25. Chen, L.-C., Sandmann, P., Thorne, J. D., Herrmann, C. S. & Debener, S. Association of concurrent fnirs and eeg signatures in response to auditory and visual stimuli. *Brain Topography* **28**, 710–725 (2015).
26. Zhou, X. *et al*. Cortical speech processing in postlingually deaf adult cochlear implant users, as revealed by functional near-infrared spectroscopy. *Trends in hearing* **22**, 2331216518786850 (2018).
27. Olds, C. *et al*. Cortical activation patterns correlate with speech understanding after cochlear implantation. *Ear and hearing* **37**(3), 160–172 (2016).
28. Fullerton, A. M. *et al*. Cross-modal functional connectivity supports speech understanding in cochlear implant users. *Cerebral Cortex* (2022).
29. Anderson, C. A., Lazard, D. S. & Hartley, D. E. Plasticity in bilateral superior temporal cortex: Effects of deafness and cochlear implantation on auditory and visual speech processing. *Hearing research* **343**, 138–149 (2017).
30. Anderson, C. A., Wiggins, I. M., Kitterick, P. T. & Hartley, D. E. Pre-operative brain imaging using functional near-infrared spectroscopy helps predict cochlear implant outcome in deaf adults. *Journal of the Association for Research in Otolaryngology* **20**(5), 511–528 (2019).
31. Sherafati, A. *et al*. Prefrontal cortex supports speech perception in listeners with cochlear implants. *elife* **11**, 75323 (2022).
32. Gomes, L. F., Vasconcelos, I. C. D., Taveira, K. V. M., Balen, S. A. & Brazorotto, J. S. Functional near-infrared spectrometry for auditory speech stimuli in cochlear implant users: a systematic literature review. *Cochlear Implants International* **25**(6), 445–458 (2024).
33. Shader, M. J., Luke, R. & McKay, C. M.: Contralateral dominance to speech in the adult auditory cortex immediately after cochlear implantation. Iscience **25**(8) (2022).
34. Shader, M. J. & Luke, R.: Auditory- and visual-evoked activity in newly implanted adult CI recipients. *Mendeley Data* https://doi.org/10.17632/377b4ff8p6. 1 (2022).
35. Steinmetzger, K., Meinhardt, B., Praetorius, M., Andermann, M. & Rupp, A. A direct comparison of voice pitch processing in acoustic and electric hearing. *NeuroImage: Clinical* **36**, 103188 (2022).
36. Oldfield, R. C. The assessment and analysis of handedness: the edinburgh inventory. *Neuropsychologia* **9**(1), 97–113 (1971).
37. Noble, W., Jensen, N. S., Naylor, G., Bhullar, N. & Akeroyd, M. A. A short form of the speech, spatial and qualities of hearing scale suitable for clinical use: The ssq12. *International journal of audiology* **52**(6), 409–412 (2013).
38. Bálint, A., Wimmer, W., Caversaccio, M., Rummel, C. & Weder, S. Brain activation patterns in normal hearing adults: An fnirs study using an adapted clinical speech comprehension task. *Hearing Research* **455**, 109155 (2025).

39. Hahlbrock, K.-H. Sprachaudiometrie: Grundlagen und Praktische Anwendung Einer Sprachaudiometrie Für Das Deutsche Sprachgebiet; 157 Abbildungen in 305 Einzeldarstellungen 9 Tabellen. Thieme,??? (1970).
40. Wagener, K., Brand, T. & Kollmeier, B. Development and evaluation of a german sentence test part iii: Evaluation of the oldenburg sentence test. *Zeitschrift Fur Audiologie* **38**, 86–95 (1999).
41. Wagener, K., Hochmuth, S., Ahrlich, M., Zokoll, M. & Kollmeier, B.: Der weibliche oldenburger satztest. In: *17th Annual Conference of the DGA*, Oldenburg, CDRom (2014).
42. Wimmer, W., Kompis, M., Stieger, C., Caversaccio, M. & Weder, S. Directional microphone contralateral routing of signals in cochlear implant users: A within-subjects comparison. *Ear and hearing* **38**(3), 368–373 (2017).
43. Gawliczek, T. *et al*. Unilateral and bilateral audiological benefit with an adhesively attached, noninvasive bone conduction hearing system. *Otology & neurotology* **39**(8), 1025–1030 (2018).
44. Wardenga, N. *et al*. Do you hear the noise? the german matrix sentence test with a fixed noise level in subjects with normal hearing and hearing impairment. *International journal of audiology* **54**(sup2), 71–79 (2015).
45. Scholkmann, F., Tachtsidis, I., Wolf, M. & Wolf, U. Systemic physiology augmented functional near-infrared spectroscopy: a powerful approach to study the embodied human brain. *Neurophotonics* **9**(3), 030801–030801 (2022).
46. Wyser, D. *et al*. Short-channel regression in functional near-infrared spectroscopy is more effective when considering heterogeneous scalp hemodynamics. *Neurophotonics* **7**(3), 035011 (2020).
47. Wyser, D. G. *et al*. Characterizing reproducibility of cerebral hemodynamic responses when applying short-channel regression in functional near-infrared spectroscopy. *Neurophotonics* **9**(1), 015004 (2022).
48. Llorach, G. *et al*. Development and evaluation of video recordings for the olsa matrix sentence test. *International Journal of Audiology* **61**(4), 311–321 (2022).
49. Zhang, Y. F., Lasfargues-Delannoy, A. & Berry, I. Adaptation of stimulation duration to enhance auditory response in fnirs block design. *Hearing Research* **424**, 108593 (2022).
50. Krueger, M. *et al*. Relation between listening effort and speech intelligibility in noise. *American Journal of Audiology* **26**(3S), 378–392 (2017).
51. Micklewright, D., St Clair Gibson, A., Gladwell, V. & Al Salman, A. Development and validity of the rating-of-fatigue scale. *Sports Medicine* **47**(11), 2375–2393 (2017).
52. Unsworth, N. & McMillan, B. D. Similarities and differences between mind-wandering and external distraction: A latent variable analysis of lapses of attention and their relation to cognitive abilities. *Acta psychologica* **150**, 14–25 (2014).
53. Stawarczyk, D., Majerus, S., Maj, M., Linden, M. & D'Argembeau, A. Mind-wandering: Phenomenology and function as assessed with a novel experience sampling method. *Acta psychologica* **136**(3), 370–381 (2011).
54. Bálint, A., Rummel, C., Caversaccio, M. & Weder, S. Three-dimensional infrared scanning: an enhanced approach for spatial registration of probes for neuroimaging. *Neurophotonics* **11**(2), 024309 (2024).
55. Bálint, A., Wimmer, W., Rummel, C., Caversaccio, M., Weder, S. An fNIRS Dataset for Multimodal Speech Comprehension in Normal Hearing Individuals and Cochlear Implant Users, https://doi.org/10.5061/dryad.crjdfn3g9.
56. Gorgolewski, K. J. *et al*. The brain imaging data structure, a format for organizing and describing outputs of neuroimaging experiments. *Scientific data* **3**(1), 1–9 (2016).
57. Luke, R. *et al*. Nirs-bids: Brain imaging data structure extended to near-infrared spectroscopy. *Scientific Data* **12**(1), 159 (2025).
58. Tucker, S. *et al*. Introduction to the shared near infrared spectroscopy format. *Neurophotonics* **10**(1), 013507 (2023).
59. Brain Imaging Data Structure Specifications for NIRS. https://bids-specification.readthedocs.io/en/stable/modality-specific-files/near-infrared-spectroscopy.html. Accessed: 2025-01-31.
60. Brain Imaging Data Structure Specifications for Modality agnostic files. https://bids-specification.readthedocs.io/en/stable/modality-agnostic-files.html. Accessed: 2025-06-18.
61. Santosa, H., Zhai, X., Fishburn, F. & Huppert, T. The nirs brain analyzir toolbox. *Algorithms* **11**(5), 73 (2018).
62. Gramfort, A. *et al*. Mne software for processing meg and eeg data. *Neuroimage* **86**, 446–460 (2014).
63. Luke, R. *et al*. Analysis methods for measuring passive auditory fnirs responses generated by a block-design paradigm. *Neurophotonics* **8**(2), 025008–025008 (2021).
64. Scholkmann, F. *et al*. A review on continuous wave functional near-infrared spectroscopy and imaging instrumentation and methodology. *Neuroimage* **85**, 6–27 (2014).
65. Saager, R. B. & Berger, A. J. Direct characterization and removal of interfering absorption trends in two-layer turbid media. *JOSA A* **22**(9), 1874–1882 (2005).
66. Cai, Z. *et al*. Evaluation of a personalized functional near infrared optical tomography workflow using maximum entropy on the mean. *Human Brain Mapping* **42**(15), 4823–4843 (2021).
67. Baker, W. B. *et al*. Modified beer-lambert law for blood flow. *Biomedical optics express* **5**(11), 4053–4075 (2014).
68. Fishburn, F. A., Ludlum, R. S., Vaidya, C. J. & Medvedev, A. V. Temporal derivative distribution repair (tddr): a motion correction method for fnirs. *Neuroimage* **184**, 171–179 (2019).
69. Cignoni, P. *et al*. Meshlab: an open-source mesh processing tool. In: *Eurographics Italian Chapter Conference*, vol. 2008, pp. 129–136 (2008). Salerno, Italy
70. Schmid, C., Wimmer, W. & Kompis, M. Bpace: A bayesian, patient-centered procedure for matrix speech tests in noise. *Trends in hearing* **27**, 23312165231191382 (2023).
71. Handwerker, D. A., Ollinger, J. M. & D'Esposito, M. Variation of bold hemodynamic responses across subjects and brain regions and their effects on statistical analyses. *Neuroimage* **21**(4), 1639–1651 (2004).
72. Polimeni, J. R. & Lewis, L. D. Imaging faster neural dynamics with fast fmri: A need for updated models of the hemodynamic response. *Progress in neurobiology* **207**, 102174 (2021).

Acknowledgements

The study was funded by the Wonderland Foundation, the Gottfried and Julia Bangerter-Rhyner Foundation, and the UniBern Research Foundation.

Author contributions

A.B.: conceptualization, methodology, formal analysis, writing-original draft. W.W.: conceptualization, methodology, formal analysis. C.R.: methodology, formal analysis. M.C.: supervision, project administration, funding acquisition. S.W.: conceptualization, methodology, project administration, funding acquisition, writing-original draft.

Competing interests

The authors declare no competing interests.

Additional information

Correspondence and requests for materials should be addressed to A.B.

Reprints and permissions information is available at www.nature.com/reprints.

Publisher's note Springer Nature remains neutral with regard to jurisdictional claims in published maps and institutional affiliations.